be excited to that state, then after 18 to 28 lifetimes the number of excited atoms is between 10^7 and 10^3, a number which in principle can produce a detectable signal. (We point out, however, that detection of emitted electrons of very low energies is by no means a trivial experimental procedure.)

We close by bringing to attention the fact that our NED formula is different from the ones found in the work of Goldberger and Watson.[5,8] Our approach consists of taking $G^d(z)=1/(z-z_0)$ with $0 \leq \mathrm{Re}z < \infty$ and $\mathrm{Im}z < 0$, the emphasis essentially being on the fact that the integration over the energy axis must start from I_1 (and not from $-\infty$) and on the expectation that for autoionizing states and especially those decaying via relativistic interactions, the observable time evolution is due to the behavior of $G^d(z)$ around E_0 only.

In conclusion, the theoretical predictions derived above suggest that there is a class of autoionizing states for which NED effects might not be prohibitively small for observation. Thus, they provide a unique opportunity to test in atomic physics the validity of a fundamental "law" of nature. A theory and application of the physical and mathematical properties of autoionizing states and their electronic structure is presented in a longer paper.[3]

[1]C. A. Nicolaides, Phys. Rev. A 6, 2078 (1972).
[2]C. A. Nicolaides, Nucl. Inst. Methods 110, 231 (1973).
[3]C. A. Nicolaides and D. R. Beck, Phys. Rev. A (to be published).
[4]E.g., P. Feldman and R. Novick, Phys. Rev. 160, 143 (1967); H. G. Berry, J. Desesquelles, and M. Dufay, Phys. Lett. 36A, 237 (1971); I. A. Sellin, D. J. Pegg, P. M. Griffin, and W. W. Smith, Phys. Rev. Lett. 28, 1229 (1972); K. Siegbahn *et al.*, *ESCA Applied to Free Molecules* (North-Holland, Amsterdam, 1969); W. Mehlorn, Phys. Fenn. 9, 223 (1974).
[5]M. L. Goldberger and K. M. Watson, *Collision Theory* (Wiley, New York, 1964).
[6]C. A. Nicolaides and D. R. Beck, in *Beam-Foil Spectroscopy*, edited by I. Sellin and D. Pegg (Plenum, New York, 1976), Vol. 1, p. 77.
[7]*Handbook of Mathematical Functions*, edited by M. A. Abramowitz and I. Stegun, National Bureau of Standards, Applied Mathematics Series No. 55 (U. S. Government Printing Office, Washington, D. C., 1964).
[8]M. L. Goldberger and K. M. Watson, Phys. Rev. 136, B1472 (1964).

High-Resolution Atomic Beam Study of the Helium Excimer Potentials $He_2(A, C\ ^1\Sigma_{u,g}^+)$

Bernhard Brutschy and Hellmut Haberland
Fakultät für Physik der Universität Freiburg, Freiburg, Germany
(Received 14 January 1977)

The long-range parts of the $A, C\ ^1\Sigma_{u,g}^+$ excimer potentials of the He_2 molecule have been accurately determined from high-resolution differential-cross-section measurements at the relative kinetic energy range from 18 to 140 meV. The barrier height of the intermediate maximum of the $A\ ^1\Sigma_u^+$ potentials is 47^{+2}_{-1} meV at an internuclear distance of 3.14 ± 0.05 Å. The long-range parts of the potential from the recent *ab initio* calculation by Guberman and Goddard is always 5 to 20 meV higher than the potential determined from our experiments.

The lowest electronically excited or excimer states of the rare-gas diatomic molecules have recently been studied very intensively because of the possibility of building tunable uv lasers. The simplest case is the excimer states of the He_2 molecule, from which lasing has not been observed so far, but which are of considerable theoretical and practical interest.[1,2]

We have studied the long-range parts of the $A\ ^1\Sigma_u^+$ and $C\ ^1\Sigma_g^+$ helium excimer potentials in a crossed-atomic-beam experiment. The experimental details have been described earlier.[3-6] Briefly, helium atoms of a supersonic beam of variable kinetic energy (16–250 meV) and very good velocity resolution (1 to 8%) is excited by coaxial electron impact to the two metastable states ($1s2s$, 2^1S and 2^3S). The singlet state can be quenched optically. This beam is crossed at a right angle with a beam of ground-state He atoms, and the angular distribution of the excited helium (He*) atoms is measured.

Figure 1 shows the experimental results for six different kinetic energies. The scattered flux of $He(2^1S)$ atoms is plotted against the lab scattering angle. The center-of-mass (c.m.) scattering angle is obtained by multiplying the lab angle by a factor of 2. All data points are normalized with the reading of a stationary monitor detector,

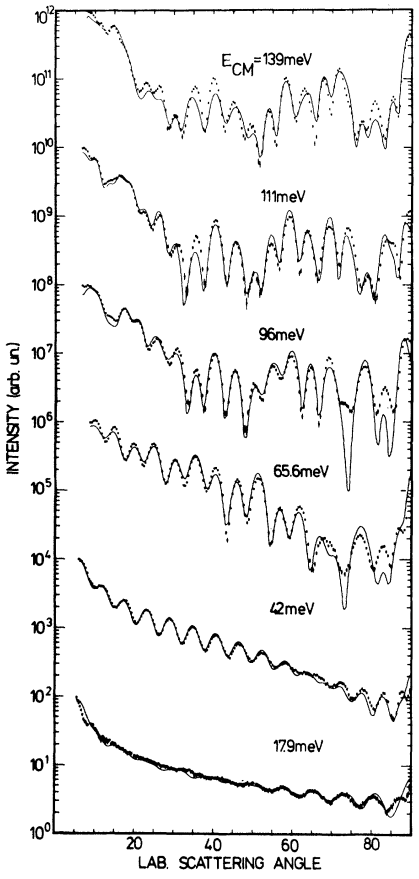

FIG. 1. Differential cross sections for He(2^1S) + He in the lab system ($\theta_{c.m.} = 2\theta_{lab}$). The regular oscillations are due to nuclear symmetry, and the irregular ones at higher energies are interferences between symmetry, symmetric-antisymmetric oscillations, orbiting and rainbow oscillations. The solid lines have been calculated from our potential.

which is placed 30° out of the plane of the two beams. Angular distributions for He(2^1S) + He have been measured before, but for only one kinetic energy and with less resolution,[7] and no interaction potential was extracted from the data.

During the scattering process the excitation energy can be exchanged several times between the two helium atoms. This exchannge is formally similar to other well-known exchange collisions. A famous example is resonant charge exchange, e.g., $H^+ + H$ or $H^+ + H^-$ where one or two electrons are exchanged, spin exchange being another example, or at much higher energies neutron exchange in $^{12}C + {}^{13}C$ scattering or π^- exchange in proton-neutron collisions.[8] In all cases, the experimentally prepared asymptotic states are not the eigenstates during the collision which leads to the multiple-exchange processes. The electronic wave function for He* + He must be either symmetric (g) or antisymmetric (u) with respect to the interchange of the excitation, and the asymptotically degenerate levels split into a symmetric ($C\ ^1\Sigma_g^+$) and an antisymmetric ($A\ ^1\Sigma_u^+$) potential. Both potentials have deep inner minima at an internuclear separation of ~1 Å, whose shapes are well known from the analyses of the emission spectrum of helium gas discharge.[2,9] Both potentials have intermediate maxima at 2–3 Å whose shapes and heights are rather uncertain. Nearly no information is available on the long-range parts of the potentials, which are so important for the understanding of collision and diffusion processes in helium gas discharges. The physical reasons for the unusual structure of the potentials has been discussed in detail by Guberman and Goddard.[2]

Loosely speaking, half of the incident flux is scattered from the symmetric potential, and the other part from the antisymmetric potential. From each potential one can calculate separately a scattering amplitude $f_g(\theta)$, $f_u(\theta)$. For the scattering of distinguishable particles, e.g., ^{4}He* from ^{3}He, one obtains a scattering amplitude $f(\theta) = \frac{1}{2}[f_g(\theta) + f_u(\theta)]$. For the scattering of identical nuclei, as in this experiment, this becomes

$$f(\theta) = \tfrac{1}{2}[f_g(\theta) + f_g(\pi - \theta) + f_u(\theta) - f_u(\pi - \theta)].$$

The minus sign in front of the exchange amplitude from the antisymmetric potential causes the differential cross section to be asymmetric with respect to 90° (45° lab).

At least four different scattering amplitudes contribute at each scattering angle. Because of this complication, and because orbiting occurs for kinetic energies above 50 meV, no inversion procedure was attempted. Flexible analytical potentials were assumed for the two potentials, and the phase shifts calculated numerically by the Numerov procedure. The parameter of the potentials were determined by the Marquardt iterative nonlinear-least-squares procedure as described earlier.[3,4] Because of the complicated interference patterns, the potential parameters had to be very near their correct values, otherwise the Marquardt routine did not converge. A rather large amount of manual adjustment of the potential parameters was therefore necessary. Those parts of the potential which are relevant to the discussion of our results are shown in Fig. 2 by the solid lines. Note the change of scale at −50 meV, which causes the apparent break in the slope of the potential. Only the out-

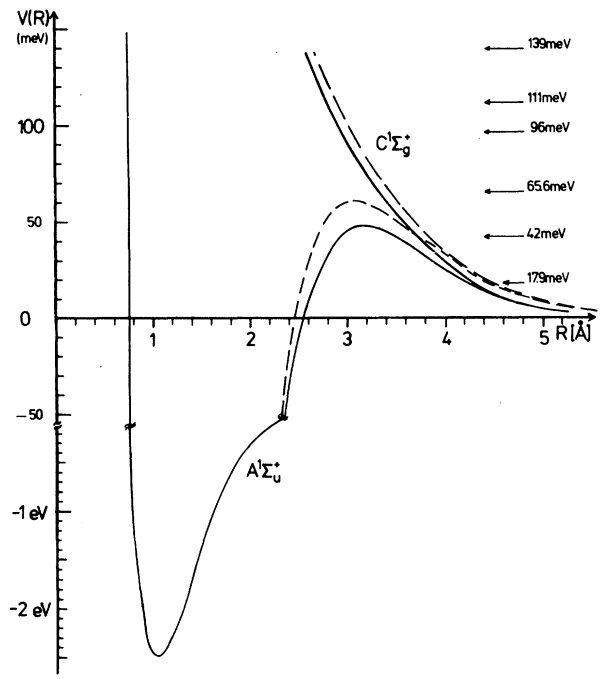

FIG. 2. The solid lines give the interaction potentials determined from the differential cross sections. The apparent break in the antisymmetric potential (V_u) is caused by the change of scale. Only the outer part of V_g is given. The dashed lines are from the *ab initio* results of Guberman and Goddard. The arrows indicate our collision energies.

er part of the $C\,^1\Sigma_g^+$ potential is given, since its intermediate maximum is too high[2] to be overcome at our collision energies, which are indicated by the horizontal arrows in Fig. 2. The differential cross sections calculated from this potential, transformed to the lab system and averaged over experimental resolution[3,4] is given by the solid lines in Fig. 1. The fit to the data is good at the lower kinetic energies, but deteriorates somewhat at higher energies. As the data are extremely sensitive to minute variations of the potential between −50 and +100 meV, the potential is believed to be rather accurate in this range, especially as it reproduces the complicated and fast-changing interference structures over a factor of 7 in kinetic energy. Some numerical values of our potentials are given in Table I. Since its analytical form is somewhat lengthy, it will be given in a future publication.[10] The potential proposed by Sando[9] has been used for $R \leq 2$ Å. The potential minima of the van der Waals attraction are at $R \geq 6$ Å, where they do not have any influence on the differential cross section, and were therefore neglected in the calculations. At $R = 6$ Å the well depth would be smaller than 1 meV. If the minimum distances are allowed to vary in the least-squares-fit routine, they are iterated to $R \approx 8$ Å. Also the 15% difference in the van der Waals constants[11] for the two potentials does not affect the differential cross sections. But this difference has a very

TABLE I. Numerical values for the long-range parts of the potentials shown in Fig. 2. For small R, the Sando potential (Ref. 9b) has been used for V_u. Our data are mostly sensitive to the potential between − 50 and +100 meV.

R (Å)	V_g (meV)	V_u (meV)
2.0		- 303.0
2.1		- 205.6
2.2		- 131.0
2.3		- 75.5
2.4		- 35.6
2.5	163.3	- 8.1
2.6	137.4	10.1
2.7	121.3	22.7
2.8	109.8	32.6
2.9	99.8	40.0
3.0	90.3	44.9
3.1	81.6	47.2
3.2	73.6	47.2
3.3	66.5	46.0
3.4	60.0	44.1
3.5	53.9	41.5
3.6	48.2	38.3
3.7	42.7	34.9
3.8	37.6	31.4
3.9	32.7	28.0
4.0	28.2	24.7
4.1	24.1	21.5
4.2	20.4	18.5
4.3	17.1	15.7
4.4	14.2	13.3
4.5	11.7	11.1
4.6	9.6	9.2
4.7	7.8	7.6
4.8	6.4	6.3
4.9	5.1	5.2
5.0	4.1	4.2

significant influence on the detailed form of the velocity distribution in our He* beam,[5] where the relative kinetic energies are much lower (10^{-2} to 10^{-5} eV).

Electronic transitions are optically forbidden only for large internuclear distances R. For finite R, dipole transitions to the $X\,^1\Sigma_g^+$ ground state are possible. They give rise to the well-known Hopfield continuum and 600-Å emission and absorption bands.[9] Only those particles can radiate which cross the barrier of the antisymmetric potential. The cross section for light emission[12] is typically 10^{-4} Å^2, which is much too small to have a noticeable influence on the differential cross sections and was therefore neglected.

Buckingham and Dalgarno[13] were the first to calculate the interaction between He(2^1S) + He. Their early calculations were refined by several authors.[2] Recently Guberman and Goddard[2] performed a generalized valence-bond (GVB) calculation for many excited He_2 states. Their results are given by the dashed lines in Fig. 2. The calculated barrier height is 60.7 meV at 3.09 Å compared to 47^{+2}_{-1} meV at 3.14 ± 0.05 Å from our determination. A GVB calculation always gives an upper limit to the exact result,[2] and in fact our results are 5 to 20 meV lower everywhere. Assuming that the atomic contribution to the correlation energy remains nearly constant for $R > 3$ Å, the authors estimate that their calculated value for the potential maximum should be reduced by 10 to 20%. The 20% value for the reduction is sufficient between 3.2 and 4 Å to roughly match the two curves. But for larger R, the discrepancy is much higher and is nearly a factor of 2 for $R > 4.9$ Å. Andresen and Kuppermann[14] have calculated differential cross sections for a potential obtained by subtracting 15% from the *ab initio* results. But this does not give a satisfactory fit to our data, especially at large scattering angles. Sando and Dalgarno[9a] have analyzed the 600-Å absorption spectra and have found a barrier height of 49 ± 10 meV at 3.1 Å, in good agreement with our results. But the long-range parts of the potentials cannot be extracted from the gas discharge spectra.

Only after the potential had been obtained was it possible to unravel the origin of all the interference structure in the differential cross sections. The very regular oscillations for energies below 80 meV result from nuclear symmetry. For the lowest two kinetic energies, the oscillations are nearly washed out for certain angular ranges. For $R > 4.2$ Å, the splitting between the potentials becomes very small ($V_g \approx V_u$), which leads to $f_g \approx f_u$. And the total scattering amplitude becomes $f(\theta) \approx \frac{1}{2}[f_g(\theta) + f_u(\theta)]$, which is the result that one would obtain for the scattering of distinguishable particles. Therefore, the symmetry oscillations are absent or severely damped.

Besides the symmetry oscillations one has at higher kinetic energies symmetric-antisymmetric oscillations, orbiting and rainbow oscillations, and their mutual interferences. The analysis of this complicated interference structure was considerably simplified or even made possible through the use of the "quantal deflection functions."[6,15] They were constructed from the numerically computed phase shifts via the relation $\theta(l+\frac{1}{2}) = 2(\eta_{l+1} - \eta_l)$, which is a straightforward generalization of the well-known semiclassical relation $\theta(l) = 2d\eta/dl$. For example, it can be shown very easily by this procedure that the large peaks at 180° (90° lab) are caused by small-angle scattering with excitation transfer.[10] And only by this procedure can the rainbow peak from the potential maximum be distinguished from all the other peaks in the differential cross sections.[10] A detailed analysis of the cross-section patterns as well as the data and analysis for He(2^3S) + He will be given elsewhere.[10]

This work was supported by the Deutsche Forschungsgemeinschaft.

[1]D. L. Lorents, Physica (Utrecht) 82C, 19 (1976); J. H. Birks, Rep. Prog. Phys. 38, 903 (1975).

[2]S. L. Guberman and W. A. Goddard, III, Phys. Rev. A 12, 1203 (1975), and references cited therein.

[3]B. Brutschy, H. Haberland, H. Morgner, and K. Schmidt, Phys. Rev. Lett. 36, 1299 (1976).

[4]B. Brutschy, H. Haberland, and K. Schmidt, J. Phys. B 9, 2693 (1976).

[5]B. Brutschy and H. Haberland, J. Phys. E 10, 90 (1977).

[6]H. Haberland and K. Schmidt, to be published.

[7]H. Haberland, C. H. Chen, and Y. T. Lee, in *Atomic Physics*, edited by S. I. Smith and G. K. Walters (Plenum, New York, 1973), Vol. 3, p. 339; C. H. Chen and Y. T. Lee, in Abstracts of the Fifth International Conference on Atomic Physics, Berkeley, California, 1976, (unpublished), p. 107.

[8]W. von Oertzen and H. G. Bohlen, Phys. Rep. C 19, 1 (1975).

[9a]K. M. Sando and A. Dalgarno, Mol. Phys. 20, 103 (1971).

[9b]K. M. Sando, Mol. Phys. 21, 439 (1971).

[9c]K. M. Sando, Mol. Phys. 23, 413 (1972).

[10]B. Brutschy and H. Haberland, unpublished; B. Brut-

schy, Ph. D. thesis, University of Freiburg, 1977 (unpublished).
[11]K. M. Sando and G. A. Victor, J. Chem. Phys. 55, 5421 (1971).
[12]A. V. Phelps, Phys. Rev. 99, 1307 (1955); H. S. W. Massey, *Electronic and Ionic Impact Phenomena* (Clarendon, Oxford, 1971), Vol. III, p. 1879.
[13]R. A. Buckingham and A. Dalgarno, Proc. Roy. Soc. London, Ser. A 213, 506 (1952).
[14]B. Andresen and A. Kuppermann, Mol. Phys. 30, 997 (1975).
[15]N. K. Glendenning, Rev. Mod. Phys. 47, 659 (1975).

Effect of Resonances on the Near-Threshold Electron Detachment Cross Sections of F^-†

Stephan Ormonde
Quantum Systems, Inc., Albuquerque, New Mexico 87108
(Received 25 May 1976)

Very narrow (~2 meV) ^1D and ^1P shape resonances above the ground state of atomic fluorine lead to electron and photon near-threshold F^- detachment cross sections of approximately $(2-3)\times10^{-15}$ and 4×10^{-14} cm^2, respectively, and could affect the F-atom production rates in the relativistic-electron-beam H_2/F_2 lasers.

I report the first use of the multiconfiguration close-coupling (MCC) formalism[1] in the problem of low-energy-electron impact detachment of negative atomic ions. During calculations of low-energy-electron impact ionization of the negative atomic fluorine ion, I found a very narrow (Γ ~0.002 eV) ^1D shape resonance in the elastic cross section at 0.009 eV above the F ground state. This resonance causes high near-threshold values of the electron and photon detachment cross sections of F^-.

There have been several studies of electron impact ionization of negative atomic ions[2] but, with two exceptions,[2a,2g] only H^- was treated; and, even for this case, no unique prescription for the near-threshold detachment process has yet evolved. References 2a and 2g contain, to my knowledge, the most exhaustive theoretical treatments of the electron detachment problem for other atoms (Na^-, Cl^-, Hg^-, and O^-) to this date. Finite attachment (detachment) cross sections to outer s or p orbitals were discussed by Massey and Smith[2a] and the detachment cross section of weakly bound p electrons in O^- was, indeed, found to be large close to threshold by Wanatabe and Miida.[2g] The Bethe-Born approximation has been shown to compare reasonably with the experimental detachment cross section in O^- for energies of 20–50 eV, but not well at lower energies, and to lead to predictions at variance with experimental data for H at higher energies.[2h]

The present study was stimulated by estimates of energy deposition in atmospheric-pressure, relativistic-electron-beam–pumped H_2/F_2 mixtures,[3] according to which the initial free-fluorine production rate could be dominated, on nanosecond time scales, by the resonant dissociative process $e+F_2\rightarrow F_2^-\rightarrow F+F^-$ (if the F_2^- state had a width of 2 eV) and that F^- formation could also contribute if the electron detachment cross section were as large as 7×10^{-15} cm^2. Detachment cross sections of such magnitude in F^- are perhaps doubtful because they imply an overestimation of available experimental data for H^- and O^- by factors of 10 and 70, respectively.[3b] I shall discuss the e-F_2^- system at a later date, and here present results for e-F^-.

In the Born approximation, the detachment cross section $\sigma^d(E)$, is given by[2a]

$$\sigma^d(E)=\frac{m^2}{2\pi\hbar^4}\int_0^{k_{\max}}\iint d\Omega\, d\Omega'\kappa^2|M_{\kappa,k}|^2 d\kappa, \tag{1a}$$

with

$$M_{\kappa,k}=\frac{4\pi}{K^2}\int\psi_0\psi_\kappa e^{i\vec{K}\cdot\vec{r}}d\tau, \tag{1b}$$

$$\psi_\kappa=\sum F_s(r)P_s(\cos\theta)i^s(2s+1),$$

so that

$$\begin{aligned}\int|M_{\kappa,k}|^2d\Omega'=\frac{32\pi^4}{3K}\{&[\int_0^\infty F_0P_{2p}(r)J_{3/2}(Kr)r^{3/2}dr]^2\\&+2[\int_0^\infty F_2P_{2p}(r)J_{3/2}(Kr)r^{3/2}dr]^2\\&+[\int_0^\infty F_1P_{2p}(r)J_{1/2}(Kr)r^{3/2}dr]^2\}\\&+\cdots,\end{aligned} \tag{1c}$$

where P_{2p} is the orbital of the bound $2p$ electron and the other quantities are as in Ref. 2a.

The close-coupling approximation can be applied to this problem just as for electron impact ionization of neutral atomic hydrogen,[4] and photo-